# Synthesis of hollow CuO/ZnO/Al$_2$O$_3$ composite microspheres for catalysing carbon dioxide hydrogenation

*Hai-feng Tian, Lei Yu, Jian Ding, Fei Zha ✉, Xiao-hua Tang, Yue Chang*

*College of Chemistry & Chemical Engineering, Northwest Normal University, Lanzhou 730070, Gansu, People's Republic of China*
✉ *E-mail: zhafei@nwnu.edu.cn*

Homogeneous hollow CuO–ZnO–Al$_2$O$_3$ microspheres, which were synthesised, used carbonaceous saccharide as a template by the hydrothermal treatment at 180°C. The hollow microspheres structure of composite metal oxides was characterised by the methods of X-ray powder diffraction, thermogravimetric analysis, scanning electron microscopy, transmission electron microscopy and N$_2$ adsorption–desorption isothermal. In the evaluation of the hydrogenation of carbon dioxide, the synthesised hollow CuO/ZnO/Al$_2$O$_3$ composite microspheres exhibited higher selectivity and yield of methanol than CuO/ZnO/Al$_2$O$_3$ prepared by a co-precipitation method. An optimum yield of methanol of 15.3% with the 24.7% CO$_2$ per pass conversion was obtained under the reaction conditions of pressure at 3.0 MPa, space velocity at 1800 ml $g_{cat}^{-1}$ h$^{-1}$, the volume ratio of CO$_2$/H$_2$ at 1:3 and temperature at 262°C.

**1. Introduction:** In recent years, carbon dioxide has become the focus of much attention because of the implication of its emissions on the problem of climate change, however, it also turned out to be a strategic carbon resource [1–3]. Thus, complete or partial recycling of CO$_2$ through its hydrogenation to high-energy density liquid fuels appears to be a very attractive approach. As a result, catalytic CO$_2$ hydrogenation reactions to methanol, higher alcohols and gasoline have received much renewed attention [4–7]. Particularly, the production of methanol is the key to platform at present chemical fuel and chemical infrastructures [8–10]. Synthesis of methanol from CO$_2$ and H$_2$ has been known and practiced since at least the 1930s and is a promising route to sustainability due to the potentially large demand for methanol [11, 12]. For methanol synthesis, copper base catalyst (CuO–ZnO) is the most common catalyst [13, 14]. At the same time, some additives, such as Zr [15], Al [16], Ce [17], Ga [15], Cr [18] and Ti [19] were added to the copper base catalyst to improve its performance. In recent years, In$_2$O$_3$/ZrO$_2$ [20] catalysts were reported for hydrogenation of CO$_2$ to methanol. However, CuO/ZnO/Al$_2$O$_3$ (CZA) catalysts showed that very high catalytic activity in all catalysts for hydrogenation of CO$_2$ to methanol. The activity of the CZA catalyst was improved with the increase of CuO species dispersion, which depends mainly on its composition and preparation method [4].

Knowledge of the structure of the active site is crucial for understanding and improving the properties of catalysts [21]. For example, CuO nanobelts exposing the (011) planes more easily release oxygen from the surface lattice, so it is more active than CuO nanoparticles with the close-packed (111) planes [22]. So far, only several examples of multi-component metal nanocrystals and semiconductor oxide nanocrystals have been demonstrated, but the role of shape controlled at the materials interface, which is the common feature in practical metal-supported catalysts, has not yet been known [23]. The synthesis of hollow nanospheres has attracted considerable attention because of their potential applications in catalyst supports, fuel cells, gas storage and separation, which result from their unique features, such as high surface-to-volume ratio, high structural stability, uniform size and low density [24]. Compared with organic hollow sphere, inorganic hollow sphere materials were widely used in the optical, magnetic, electrical, thermal, optoelectronic, electrochemical, catalytic properties, mechanical and photoelectrochemical [25–30].

Instead of fabricating the hollow spheres by a multistep process that involves the formation, isolation and purification of the carbon sphere, coating of the sacrificial cores with the metal oxide precursors, and subsequent removal of the carbon cores via calcinations. In the present contribution, metal salts were added directly to the aqueous carbohydrate to form homogeneous hollow CuO–ZnO–Al$_2$O$_3$ microspheres, which showed that this promising approach could be even more simplified and generalised. The homogeneous hollow CuO–ZnO–Al$_2$O$_3$ microspheres could be expected to be a dramatically beneficial carbon dioxide hydrogenation catalyst.

**2. Experiment:** All reagents were of analytical grade (purchased from Tianjin Kaixi chemical industry company) and were used as raw materials without further purification. Ultrapure water was adopted throughout the experiment.

2.1. Catalyst preparation: First, 15.0 mmol of water-soluble metal precursors of Cu(NO$_3$)$_2$·3H$_2$O, Zn(NO$_3$)$_2$·6H$_2$O and Al(NO$_3$)$_3$·9H$_2$O with a mass ratio of 6/3/1 were dissolved in 40 ml of distilled water. Then, the above solution was mixed immediately with 10 ml glucose aqueous solution (0.75 mol/l) in Teflon-lined stainless autoclave. It was heated in an oven to 180°C for 24 h, then cooled to room temperature naturally. After filtration, the solid was washed several times with distilled water and ethanol, respectively. The solid was dried in the vacuum oven at 60°C for 6 h. The metal oxides–carbon composites were calcined in air at 600°C (heating rate of 4°C/min) for 2 h to remove the carbon cores, leading to hollow CuO/ZnO/Al$_2$O$_3$ (HCZA) spheres. Based on the evidence obtained from experimental results and references [31], the formation of HCZA was elaborated in Fig. 1. The tri-component CuO–ZnO–Al$_2$O$_3$ (CZA) was prepared by a conventional co-precipitation method with hydrated metal nitrates (Cu(NO$_3$)$_2$·3H$_2$O, Zn(NO$_3$)$_2$·6H$_2$O and Al(NO$_3$)$_3$·9H$_2$O) were used as metal precursors [32] and the mass ratio hydrated metal nitrates is 6: 3:1.

2.2. Catalyst characterisation: The powder X-ray diffraction (XRD) patterns were collected on a Rigaku D/Max-2400 ($\lambda = 0.1542$ Å) with Cu Kα radiation source operating at 40 KV and 60 mA to identify the phases and their crystallinity. Scanning electron microscopy (SEM) images were obtained using a JEOL JSM-5600 instrument. An
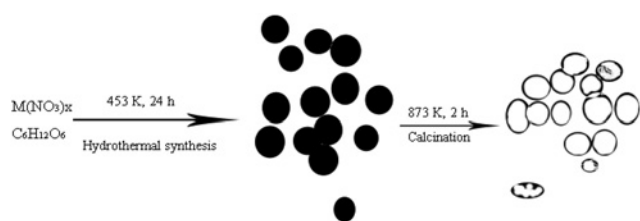
**Fig. 1** *General synthesis of hollow CuO/ZnO/Al₂O₃ composite microspheres*

Omega 912 transmission electron microscope (TEM) was also used to observe the images. Energy dispersive X-ray spectroscopy (EDS) analysis was performed by a Noran SystemSix instrument which was used to determine the elemental composition of the hollow spheres. Thermal analyses of the synthesised materials were made using the Perkin–Elmer TG/DTA-6300 thermal analyses system. The Brunauer–Emmett–Teller surface area and pore size distribution of the hollow spheres were determined by $N_2$ sorption using a Quantachrome Autosorb-1 apparatus. The pore volume was determined at a relative pressure ($P/P_o$) of 0.99.

2.3. Catalysis reaction and products analysis: The catalytic activities for the carbon dioxide hydrogenation were carried out in a stainless fix-bed reactor [33]. Before the real hydrogenation reaction test, the catalysts were reduced in a 5% $H_2$–95% $N_2$ stream at reaction temperature for 4 h. Then the gas mixture composed of 25% $CO_2$ and 75% $H_2$ with a space velocity (SV) 1800 ml $g_{cat}^{-1}$ $h^{-1}$ was allowed to flow through the catalyst bed. The reaction was operated under isothermal condition when the catalyst bed containing 0.5 g catalyst was installed in a flat-temperature zone in the reactor. Therefore, there were few radial and axial temp-gradients because of only ±1.5°C existing in the flat-temperature zone. After reaction for 1 h, the catalysts reach the steady state, the compositions of the reaction products were analysed by online gas chromatograph (Kechuang GC 900A, China) with a thermal conductivity detector using ethyl silicone packed column (TDX501, 1.5 m × 3 mm) and Porapak Q packed column (2 m × 3 mm). The $CO_2$ conversion and products distribution were calculated to use the area normalisation method [34].

## 3. Results and discussion

3.1. Analysis of XRD: Fig. 2 shows the diffraction patterns of the particles before and after calcination. The carbon sphere was formed from aqueous glucose by hydrothermal method [35, 36], so a few crystalline peaks ($2\theta = 5°-30°$) are attributable to amorphous carbon before calcination. The Cu peaks indicate, the formation of elemental copper in the samples which becomes copper oxide during calcinations. Al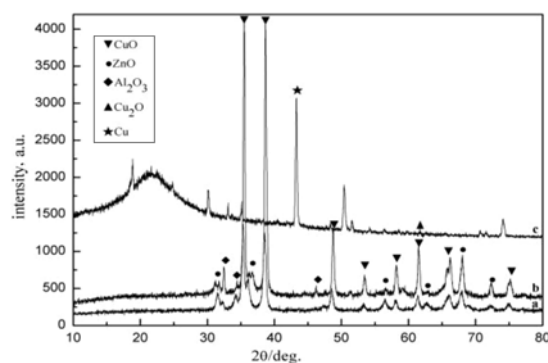l the hollow microspheres are composed of crystalline CuO, ZnO and Al₂O₃ without other phases present after calcination [32]. The relative intensity of CuO, ZnO and Al₂O₃ peaks increase in hollow spheres due to the high purity and crystallinity of metal oxides in the capsule, compared with the same peak in CZA prepared by a conventional co-precipitation method.

3.2. Thermogravimetric analysis: Thermogravimetric analysis results (shown in Fig. 3) suggest no significant decomposition occurred. The 0.2% of weight loss, which is assigned to desorption of surface-absorbed $H_2O$, observed after heating to 800°C, confirming that carbon template could be removed completely. The endothermic peak after 720°C is partial due to the lattice transformation and metal sintering. It is known that one of the biggest challenges for heterogeneous catalysts is the minimisation of thermal agglomeration of the catalytic centres at elevated temperatures, which results in significant degradation of the apparent activity. The interior surface of the hollow capsules is most likely free from thermal agglomeration since it is isolated from the other capsules by the exterior surface [37]. The very high $CO_2$ hydrogenation activity of the hollow capsules can be ascribed to the highly active and agglomeration-free interior surface.

3.3. Analysis of $N_2$ adsorption-desorption isotherms and pore size distribution: The $N_2$ adsorption–desorption isotherms and pore size distribution are shown in Fig. 4. The specific surface area, pore volume and average pore diameter of the tricomponent CuO–ZnO–Al₂O₃ are 48.03 m²/g, 0.159 cm³/g and 0.756 nm, respectively. HCZA is composed of nanoparticles of the corresponding metal oxides and a high surface area can be expected. However, the specific surface area, pore volume and average pore diameter of hollow spheres are 21.50 m²/g, 0.207 cm³/g and 0.757 nm, respectively. When the carbon microspheres were ultrasonically treated for 15 min in ethanol at room temperature before the roasting, the specific surface area, pore volume of HCZA could be increased to 58.61 m²/g, 0.330 cm³/g, respectively. The results show that the carbon microspheres are fully dispersed after ultrasonic treatment of ethanol, which reduces the agglomeration and sintering caused by agglomeration after calcination, increases the specific surface area, enhances the gas absorption and storage capacity, and provides more surface metal active sites.

3.4. Analysis of SEM images: To obtain detailed information about microstructure and morphology of the multiple metal oxides, SEM was carried out and the images are shown in Fig. 5. Apparently, the diameter of the hollow sphere is about 500–2000 nm, the spheres shell surface is not smooth and are composed of aggregated nanoparticles of multiple metal oxides. It is interesting to note that the aggregation of these NPs can produce inherent porosity which creates numerous nanoscale channels for chemical moieties
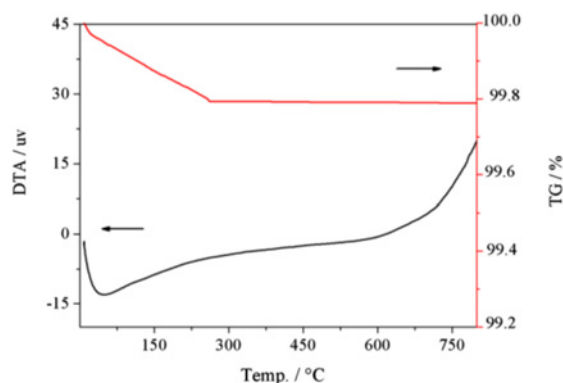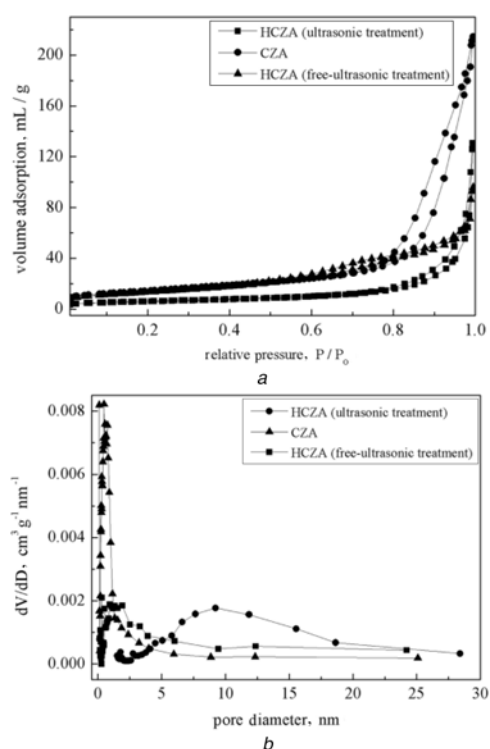


**Fig. 2** *XRD patterns of (a) CZA, (b) HCZA and (c) carbon spheres saturated with metal ions*



**Fig. 3** *TG and DTA curve of HCZA*

Fig. 4 *$N_2$ adsorption–desorption isotherms and pore size distribution*



Fig. 5 *SEM images of HCZA*



Fig. 6 *TEM images of HCZA and EDS analysis*

**Table 1** Catalytic performance of the CZA and HCZA

| Catalyst | Conversion, % | Yield, % | Selectivity, % | |
| --- | --- | --- | --- | --- |
| | $CO_2$ | MeOH | MeOH | CO |
| CZA | 19.6 | 11.7 | 59.7 | 40.3 |
| HCZA | 24.7 | 15.3 | 61.8 | 38.2 |

Reaction conditions: $P = 3.0$ MPa, $SV = 1800$ ml $g_{cat}^{-1}$ $h^{-1}$, $CO_2/H_2$ (1: 3) and $T = 262°C$.

3.5. TEM images and EDS analysis: The obtained hollow spheres were further investigated by means of TEM. Fig. 6 displays the micrographs and components of HCZA. All micrographs show spherical hollow structures, even though some rough edges on the surface are clearly observed. The shell with some inherent porosity is composed of aggregated nanoparticles of the metal oxides and thickness of the shell is around 30 nm. Line scans of energy dispersive X-ray microanalysis (EDS) indicate that HCZA has the mass loading of metal of Cu/Zn/Al = 5.5: 2.9:1.4. It is very similar to its original bulk ratio ($CuO/ZnO/Al_2O_3$ in a mass ratio of 6/3/1). The results suggest the possibility of producing hollow composite metal oxides through a simple one-step hydrothermal synthesis by using carbonaceous saccharide microspheres as a template. These sacrificial cores of carbonaceous saccharide microspheres with functional groups and have reactive surfaces, which facilitates the absorption of cationic metal ions and the precipitation of metal precursors, are generated by the hydrothermal treatment of glucose aqueous solutions [39].

3.6. The activity for the synthesis of methanol: The activities of the CZA and HCZA for $CO_2$ hydrogenation were detected when the reaction pressure was at 3.0 MPa, temperature at 262°C, SV at 1800 ml $g_{cat}^{-1}$ $h^{-1}$ and $CO_2/H_2$ ratio at 1:3. It can be seen from Table 1 that a hollow sphere catalyst can increase the
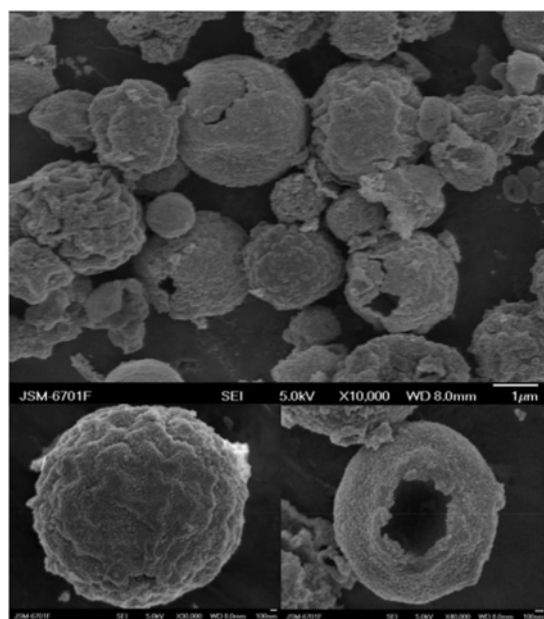
travelling between the interior cavity and exterior space, thus making the hollow spheres particularly suitable for further studies in adsorption and catalytic applications [38]. The hole with diameter of about 250 nm can be seen evidently in the microsphere. Various opened hollow spheres can be also observed, but the hollow sphere wall has not seriously damaged. It can because of the high-speed releases of carbon dioxide or the ultrasonic wave conduction on the samples [37]. It can be seen from the broken hollow sphere shell that the product has a hollow cavity. The hollow cavity is connected with the air gap from which the outside passes through the hollow sphere shell.
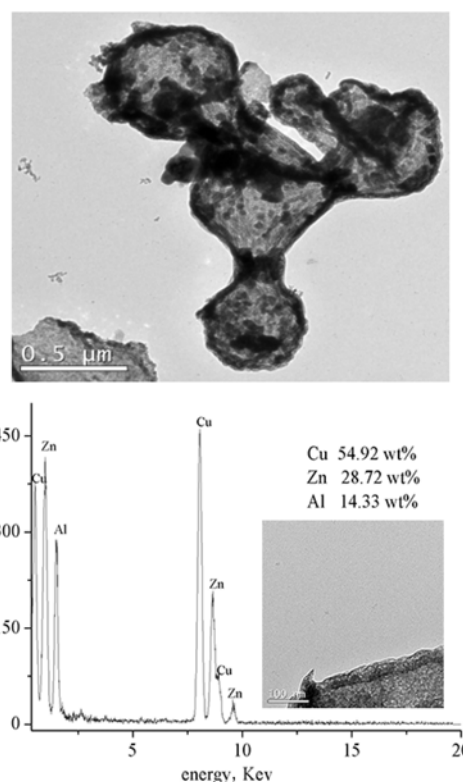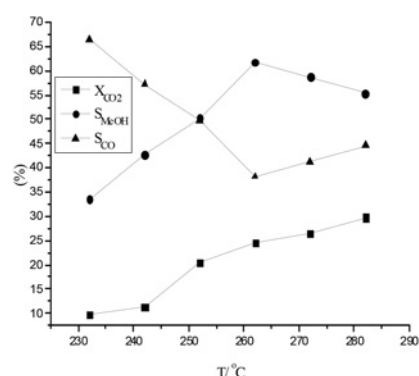
**Fig. 7** *Effect of temperature on the activity of $CO_2$ hydrogenation to MeOH. Reaction conditions: P = 3.0 MPa, SV = 1800 ml $g_{cat}^{-1} h^{-1}$, $CO_2/H_2$ = 1:3*



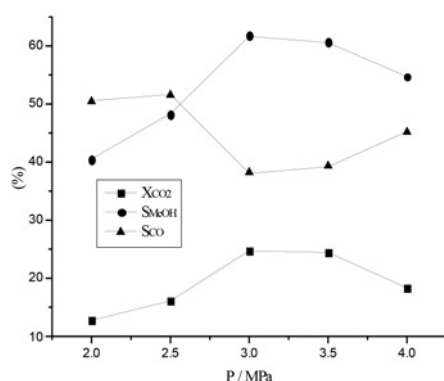**Fig. 8** *Effect of pressure on the activity of $CO_2$ hydrogenation to MeOH. eaction conditions: T = 262°C, SV = 1800 ml $g_{cat}^{-1} h^{-1}$, $CO_2/H_2$ = 1:3*

conversion of carbon dioxide and yield methanol and maintain the near-zero formation of the unexpected alkanes by-product. The hollow HCZA catalyst can provide metal activity site of the inner and outer surface and promoted the rapid diffusion of the reactants and products. It is favourable for the conversion of $CO_2$ and the generation of MeOH in the hydrogenation of carbon dioxide. Therefore, this hollow sphere of multivariate metal oxide can be regarded as an excellent methanol synthesis catalyst.

3.7. Effect of reaction temperature: The catalytic performance of HCZA hollow sphere catalysts were investigated in the hydrogenation of carbon dioxide to methanol at various reaction temperatures and the results are shown in Fig. 7. The conversion of $CO_2$ increases with the increase in reaction temperature from 232 to 262°C. The low conversion of $CO_2$ at low temperature was due to the competitive adsorption between CO and $CO_2$ on the metallic function of the catalyst since methanol formation from hydrogenation of carbon monoxide which was formed from the reverse water gas shift reaction [40]. The increase of $CO_2$ conversion and decrease of MeOH selectivity with temperature above 262°C are due to the fact that the reverse water gas shift reaction is favourable with an increase of temperature. Compared with the Cu-based catalyst system by a co-precipitation, the decrease rate of MeOH selectivity was great slow. It owes to the special hollow structure, which makes its surface separate from each other and provides high heat dissipation throughout the catalyst body preventing hot spot formation, avoiding the sinter and removal of copper activity centre [41]. Therefore, the hollow HCZA sphere is a good sinter-resistant catalytic for $CO_2$ hydrogenation to MeOH [42].

3.8. Effect of reaction pressure: MeOH synthesis in the pressure range of 2.0–4.0 MPa was also investigated. The relationship

between the reaction pressure and $CO_2$ conversion and methanol selectivity are shown in Fig. 8. At a pressure of 2.0 MPa, the $CO_2$ conversion is just 12.8%. When the pressure is increased to 3.0 MPa, the $CO_2$ conversion is increased to 24.7%. The methanol selectivity is also shown similar trends that it is of 40.5% at 2.0 MPa and is 61.8% at 3.0 MPa. The equilibrium for methanol formation is favoured at high pressures [43], however, we found that there is no noticeable improvement of $CO_2$ conversion and MeOH selectivity when the pressure is increased from 3.0 to 3.5 MPa and the $CO_2$ conversion and MeOH selectivity dramatic decreases when the pressure is increased from 3.5 to 4.0 MPa, mainly because hollow sphere structure is broken leading to the decrease of catalyst activity when the pressure is increased >3.5 MPa.

**4. Conclusions:** The hollow structure composite metal oxide microsphere was prepared successfully when glucose was mixed with metal salt solutions by hydrothermal reaction. The hollow HCZA catalyst can provide metal activity site at the inner and outer surface and promotes the rapid diffusion of the reactants and products. It is favourable for the conversion of $CO_2$ and the generation of MeOH in the hydrogenation of carbon dioxide. Hollow structure catalyst has strong resistance to sintering. The HCZA displayed superior catalytic performances compared to $CuO/ZnO/Al_2O_3$ prepared by a co-precipitation method, indicating the potential application of the hollow structured materials in the hydrogenation of carbon dioxide to methanol reaction.

**6 References**

[1] Federsel C., Jackstell R., Beller M.: 'State-of-the-art catalysts for hydrogenation of carbon dioxide', *Angew. Chem. Int. Ed.*, 2010, **49**, (36), pp. 6254–6257

[2] Chen C., Ayvalı T., Suo H., ET AL.: '$CO_2$ hydrogenation to methanol over catalysts derived from single cationic layer CuZnGa LDH precursors', *ACS Catal.*, 2018, **8**, (5), pp. 4390–4401

[3] Dang S., Gao P., Liu Z., ET AL.: 'Role of zirconium in direct $CO_2$ hydrogenation to lower olefins on oxide/zeolite bifunctional catalysts', *J. Catal.*, 2018, **364**, pp. 382–393

[4] Arena F., Barbera K., Italiano G., ET AL.: 'Synthesis, characterization and activity pattern of Cu-ZnO/ZrO$_2$ catalysts in the hydrogenation of carbon dioxide to methanol', *J. Catal.*, 2007, **249**, (2), pp. 185–194

[5] Chen H.-B., Liao D.-W., Yu L.-J., ET AL.: 'Influence of trivalent metal ions on the surface structure of a copper-based catalyst for methanol synthesis', *Appl. Surf. Sci.*, 1999, **147**, (1–4), pp. 85–93

[6] Li S., Guo H., Luo C., ET AL.: 'Effect of iron promoter on structure and performance of K/Cu-Zn catalyst for higher alcohols synthesis from $CO_2$ hydrogenation', *Catal. Lett.*, 2013, **143**, (4), pp. 345–355

[7] Tursunov O., Kustov L., Tilyabaev Z.: 'Methanol synthesis from the catalytic hydrogenation of $CO_2$ over CuO-ZnO supported on aluminum and silicon oxides', *J. Taiwan Inst. Chem. Eng.*, 2017, **78**, pp. 416–422

[8] Liu X.-M., Lu G.-Q., Yan Z.-F., ET AL.: 'Recent advances in catalysts for methanol synthesis via hydrogenation of CO and $CO_2$', *Ind. Eng. Chem. Prod. Res.*, 2003, **42**, (25), pp. 6518–6530

[9] Naik S.-P., Du H., Wan H., ET AL.: 'A comparative study of ZnO-CuO-Al$_2$O$_3$/SiO$_2$-Al$_2$O$_3$ composite and hybrid catalysts for direct synthesis of dimethyl ether from syngas', *Ind. Eng. Chem. Prod. Res.*, 2008, **47**, (23), pp. 9791–9794

[10] Li Z., Zuo Z., Huang W., ET AL.: 'Research on Si-Al based catalysts prepared by complete liquid-phase method for DME synthesis in a slurry reactor', *Appl. Surf. Sci.*, 2011, **257**, (6), pp. 2180–2183

[11] Doss B., Ramos C., Atkins S.: 'Optimization of methanol synthesis from carbon dioxide and hydrogen: demonstration of a pilot-scale carbon-neutral synthetic fuels process', *Energy Fuels*, 2009, **23**, (9), pp. 4647–4650

[12] Liao S.-Y., Jiang D.-M., Cheng Q., ET AL.: 'Effect of methanol addition into gasoline on the combustion characteristics at relatively low temperatures', *Energy Fuels*, 2006, **20**, (1), pp. 84–90

[13] Abu-Dahrieh J., Rooney D., Goguet A., ET AL.: 'Activity and deactivation studies for direct dimethyl ether synthesis using CuO-ZnO-Al$_2$O$_3$ with NH$_4$ZSM-5, HZSM-5 or γ-Al$_2$O$_3$', *Chem. Eng. J.*, 2012, **203**, pp. 201–211

[14] Sun Q., Zhang Y.-L., Chen H.-Y., ET AL.: 'A novel process for the preparation of Cu/ZnO and Cu/ZnO/Al$_2$O$_3$ ultrafine catalyst: structure, surface properties, and activity for methanol synthesis from CO$_2$+ -H$_2$', *J. Catal.*, 1997, **167**, (1), pp. 92–105

[15] Ladera R., Pérez-Alonso F.-J., González-Carballo J.-M., ET AL.: 'Catalytic valorization of CO$_2$ via methanol synthesis with Ga-promoted Cu-ZnO-ZrO$_2$ catalysts', *Appl. Catal., B*, 2013, **142**, pp. 241–248

[16] Dibenedetto A., Angelini A., Stufano P.: 'Use of carbon dioxide as feedstock for chemicals and fuels: homogeneous and heterogeneous catalysis', *Indian J. Chem. Technol.*, 2014, **89**, (3), pp. 334–353

[17] Angelo L., Kobl K., Parkhomenko K., ET AL.: 'Study of CuZnMOx oxides (M = Al, Zr, Ce, CeZr) for the catalytic hydrogenation of CO$_2$ into methanol', *C.R. Chim.*, 2015, **18**, (3), pp. 250–260

[18] Saito M., Fujitani T., Takeuchi M., ET AL.: 'Development of copper/zinc oxide-based multicomponent catalysts for methanol synthesis from carbon dioxide and hydrogen', *Appl. Catal., A*, 1996, **138**, (2), pp. 311–318

[19] Xiao J., Mao D., Guo X., ET AL.: 'Methanol synthesis from CO$_2$ hydrogenation over CuO-ZnO-TiO$_2$ catalysts: the influence of TiO$_2$ content', *Energy Technol.*, 2015, **3**, (1), pp. 32–39

[20] Martin O., Martín A.-J., Mondelli C., ET AL.: 'Indium oxide as a superior catalyst for methanol synthesis by CO$_2$ hydrogenation', *Angew. Chem. Int. Ed.*, 2016, **55**, (21), pp. 6261–6265

[21] Greeley J.-P.: 'Active site of an industrial catalyst', *Science*, 2012, **336**, (6083), pp. 810–811

[22] Zhou K., Wang R., Xu B., ET AL.: 'Synthesis, characterization and catalytic properties of CuO nanocrystals with various shapes', *Nanotechnology*, 2006, **17**, (15), p. 3939

[23] Liao F., Huang Y., Ge J., ET AL.: 'Morphology-dependent interactions of ZnO with Cu nanoparticles at the materials' interface in selective hydrogenation of CO$_2$ to CH$_3$OH', *Angew. Chem. Int. Ed.*, 2011, **50**, (9), pp. 2162–2165

[24] Zhang H., Zhu Q., Zhang Y., ET AL.: 'One-pot synthesis and hierarchical assembly of hollow Cu$_2$O microspheres with nanocrystals-composed porous multishell and their gas-sensing properties', *Adv. Funct. Mater.*, 2007, **17**, (15), pp. 2766–2771

[25] Lou X.-W., Archer L.-A., Yang Z.: 'Hollow micro-nanostructures: synthesis and applications', *Adv. Mater.*, 2008, **20**, (21), pp. 3987–4019

[26] Rogach A.-L., Gaponik N., Lupton J.-M., ET AL.: 'Light-emitting diodes with semiconductor nanocrystals', *Angew. Chem. Int. Ed.*, 2008, **47**, (35), pp. 6538–6549

[27] Lemaire B.-J., Davidson P., Ferré J., ET AL.: 'Outstanding magnetic properties of nematic suspensions of goethite (α-FeOOH) nanorods', *Phys. Rev. Lett.*, 2002, **88**, (12), p. 125507

[28] Shan Z.-W., Adesso G., Cabot A., ET AL.: 'Ultrahigh stress and strain in hierarchically structured hollow nanoparticles', *Nat. Mater.*, 2008, **7**, (12), p. 947

[29] Wen B., Sader J.-E., Boland J.-J.: 'Mechanical properties of ZnO nanowires', *Phys. Rev. Lett.*, 2008, **101**, (17), p. 175502

[30] Li K., Wang X., Zhang F., ET AL.: 'Electronegativity identification of novel superhard materials', *Phys. Rev. Lett.*, 2008, **100**, (23), p. 235504

[31] Li X.-L., Lou T.-J., Sun X.-M., ET AL.: 'Highly sensitive WO$_3$ hollow-sphere gas sensors', *Inorg. Chem.*, 2004, **43**, (17), pp. 5442–5449

[32] Wulff G.: 'Molecular imprinting in cross-linked materials with the aid of molecular templates-a way towards artificial antibodies', *Angew. Chem. Int. Ed.*, 1995, **34**, (17), pp. 1812–1832

[33] Erena J., Garona R., Arandes J.-M., ET AL.: 'Effect of operating conditions on the synthesis of dimethyl ether over a CuO-ZnO-Al$_2$O$_3$/NaHZSM-5 bifunctional catalyst', *Catal. Today*, 2005, **107**, pp. 467–473

[34] Zha F., Ding J., Chang Y., ET AL.: 'Cu-Zn-Al oxide cores packed by metal-doped amorphous silica–alumina membrane for catalyzing the hydrogenation of carbon dioxide to dimethyl ether', *Ind. Eng. Chem. Res.*, 2011, **51**, (1), pp. 345–352

[35] Liu R., Tian H., Yang A., ET AL.: 'Preparation of HZSM-5 membrane packed CuO-ZnO-Al$_2$O$_3$ nanoparticles for catalysing carbon dioxide hydrogenation to dimethyl ether', *Appl. Surf. Sci.*, 2015, **345**, pp. 1–9

[36] Wen Z., Wang Q., Zhang Q., ET AL.: 'Hollow carbon spheres with wide size distribution as anode catalyst support for direct methanol fuel cells', *Electrochem. Commun.*, 2007, **9**, (8), pp. 1867–1872

[37] Mandal S., Sathish M., Saravanan G., ET AL.: 'Open-mouthed metallic microcapsules: exploring performance improvements at agglomeration-ree interiors', *J. Am. Chem. Soc.*, 2010, **132**, (41), pp. 14415–14417

[38] Luo M., Liu Y., Hu J., ET AL.: 'General strategy for one-pot synthesis of metal sulfide hollow spheres with enhanced photocatalytic activity', *Appl. Catal., B*, 2012, **125**, pp. 180–188

[39] Sun X., Li Y.: 'Ga$_2$o$_3$ and GaN semiconductor hollow spheres', *Angew. Chem. Int. Ed.*, 2004, **116**, (29), pp. 3915–3919

[40] Li Q., Xin C., Lian P.: 'The synthesis and application of CuO-ZnO/HZSM-5 catalyst with core-shell structure', *Pet. Sci. Technol.*, 2012, **30**, (21), pp. 2187–2195

[41] Bartholomew C.-H.: 'Mechanisms of catalyst deactivation', *Appl. Catal. A, Gen.*, 2001, **212**, (1–2), pp. 17–60

[42] Dai Y., Lim B., Yang Y., ET AL.: 'A sinter-resistant catalytic system based on platinum nanoparticles supported on TiO$_2$ nanofibers and covered by porous silica', *Angew. Chem. Int. Ed.*, 2010, **49**, (44), pp. 8165–8168

[43] Waugh K.-C.: 'Methanol synthesis', *Catal. Lett.*, 2012, **142**, (10), pp. 1153–1166